Efficient transformation of cyclohexanone to ϵ-caprolactone in the oxygen-aldehyde system over single-site titanium BEA zeolite

Katarzyna Pamin, Jacek Gurgul, Grzegorz Mordarski, Yannick Millot, Jean-Philippe Nogier, Laetitia Valentin, Stanislaw Dzwigaj

Efficient transformation of cyclohexanone to ε-caprolactone in the oxygen-aldehyde system over single-site titanium BEA zeolite

Katarzyna Pamin[1,*], Jacek Gurgul[1], Grzegorz Mordarski[1], Yannick Millot[2], Jean-Philippe Nogier[2], Laetitia Valentin[2], and Stanislaw Dzwigaj[2,*]

[1]Jerzy Haber Institute of Catalysis and Surface Chemistry, Polish Academy of Sciences, Niezapominajek 8, PL-30239 Krakow, Poland

[2]Laboratoire de Réactivité de Surface, Sorbonne Université-CNRS, UMR 7197, 4 Place Jussieu, Case 178, F-75252 Paris, France

*Corresponding authors:

Stanislaw Dzwigaj, e-mail: stanislaw.dzwigaj@upmc.fr,

Katarzyna Pamin, e-mail: ncpamin@cyf-kr.edu.pl,

KEYWORDS: Titanium; Beta zeolite; Baeyer-Villiger oxidation; Cycloketones; Molecular oxygen.

Abstract

Ti_xSiBEA zeolites prepared by a two-step post-synthesis method are applied in the liquid-phase Baeyer-Villiger oxidation of cyclohexanone to ε-caprolactone in the oxygen-aldehyde system. Such method of ε-caprolactone synthesis offers the application of milder reaction conditions with the catalytic system which transforms cyclic ketones into lactones in the presence of molecular oxygen and aldehyde. They are the source of *in situ* peracid formation. The Ti incorporation into SiBEA involves the formation of $Ti(IV)(OSi)_4$ as main species and small numbers of $Ti(III)(OSi)_3$-O(H)-Si sites having Brønsted and Lewis acid properties. The acidity is a key factor for efficient transformation of cyclohexanone to ε-caprolactone in the BV oxidation depending on the titanium oxidation state and environment. Among all of the studied catalysts, the highest catalytic activity is observed for $Ti_{2.0}SiBEA$ zeolite. The active catalyst of the studied BV oxidation reaction is bi-functional, possessing both the acidic and redox properties, catalyzing different reaction stages.

Introduction

The Baeyer–Villiger (BV) oxidation of cyclic ketones into lactones or ketones into esters is drawing much attention due to the formation of varied products with various functional groups necessary for manufacturing pharmaceuticals, monomers for biodegradable plastics or intermediates for fine chemicals [1]. BV oxidation is the large-scale industrial process for transformation of cyclohexanone to ε-caprolactone which is a monomer to produce polycaprolactone [2]. On the industrial scale ε-caprolactone is produced with the use of aggressive and toxic oxygen donor-like peracetic acid which makes the applied production method expensive and dangerous for natural environment. An alternative for the existing processes is a catalytic system in which cyclic ketones can be transformed into lactones in the presence of ecologically friendly reagents, such as hydrogen peroxide or molecular oxygen and aldehyde as co-catalyst.

Hydrogen peroxide is regarded as one of the weakest oxidants and its catalytic action should be reinforced by the presence of transition metal catalysts such as Pt or Pd [3]. Several transition metal catalysts were applied as catalysts with H_2O_2 as oxidant. The advantage of hydrogen peroxide is its low cost and formation of water as the only by-product. In 1978 Jacobson *et al.* [4] described the first example of the use of Mo(VI) complexes in BV oxidation with rather moderate efficiency. Rhenium complexes have been proven to be active catalysts of BV oxidation for a variety of simple cyclic ketones [5]. In the presence of tungstophosphoric acid cyclic ketones were converted to appropriate lactones with moderate selectivity [6]. Another heteropolyacid, $H_3SiW_{12}O_{40}$, supported on multi-walled carbon nanotubes demonstrated high catalytic activity in BV oxidation of a series of cyclic ketones. Heterogenization of tungstosilicic acid resulted in an easier recovery and in possible reuse of the catalyst in cyclopentanone

oxidation [7]. A particularly important group of the catalysts active in the BV oxidation are Sn-based compounds. Corma *et al.* [8] applied, for the first time, tin containing Beta zeolite for BV oxidation of saturated ketones. Due to its unique active site geometry, an excellent catalytic performance and facility of separation from the reaction mixture, it proved to be an ideal catalyst for ketones lactonization. Application of tin catalysts like Sn-exchanged hydrotalcites and their further reuse in the oxidation of cycloketones to lactones were described in [9,10]. However, it should be noted that hydrogen peroxide used in higher concentrations and in the presence of organic compounds can be unstable and harmful for the reaction vessels [3], therefore such processes require expensive protection.

Alternatively, Yamada *et al.* [11] developed a catalytic system which enables BV transformation to be carried out over Ni catalysts in the presence of molecular oxygen and sacrificial aldehyde (Mukaiyama system). This method is environmentally attractive since it utilizes the cheapest oxidizing agent – oxygen. Also, the addition of sacrificial aldehyde to the reaction mixture allows BV oxidation to proceed under mild and environmentally acceptable conditions. Moreover, in this process two useful compounds are produced, a lactone and an acid. As opposed to the classical method using hazardous peroxycarboxylic acid as common oxidant, in the Mukaiyama system peracid is formed only *in situ*. It is widely accepted [3,12] that aldehyde, in the presence of molecular oxygen, in the Mukaiyama procedure generates peracid which in turn converts cyclic ketone into lactone. BV oxidation in the Mukaiyama conditions proceeds efficiently in the presence of metal complexes via free radical chain mechanism [12]. As it was proven [13], the most beneficial catalytic system should be bi-functional. The redox properties are necessary to facilitate the autooxidation of aldehyde to peracid while Lewis acid sites participate in the activation of ketone.

Considerable attention has been devoted to the application of dioxygen as oxidant in BV oxidation. Lakk-Bogath *et al.* [14] reported on the high-valent oxoiron complex as highly selective and efficient catalyst of the oxidation of various cyclohexanones in the presence of different aldehydes as oxygen acceptors. Application of Fe-Sn-O mixed oxides in the BV oxidation of cyclohexanone also resulted in their excellent catalytic performance [15], which becomes poorer in the oxidation of aliphatic ketones. Another important group of catalysts - heteropolysalts with changing stoichiometry were employed in the BV oxidation of cyclohexanone to ε-caprolactone. Pamin *et al.* [13] demonstrated that the active catalyst of the studied BV oxidation is the bi-functional catalyst possessing both the acidic and the redox properties, which catalyzes the different reaction stages. Apart from the numerous metal complexes as catalysts in the BV oxidation, several heterogeneous catalytic systems based on the various supports have been applied. In the presence of sulphonated cobalt phthalocyanine intercalated hydrotalcite, the oxidation of various cyclic ketones proceeds with high conversion and selectivity [16,17]. BV oxidation of cyclohexanone with various oxidants in the presence of iron containing hydrotalcite-type materials revealed excellent conversion of ketone and yield to lactone for the reaction carried out in the Mukaiyama conditions [18]. To overcome the diffusion limitations of the reactants observed for the Sn-zeolite type catalysts, the mesoporous based materials were applied. For example, Fe^{3+} ions incorporated into mesoporous MCM-48 material demonstrated excellent catalytic activity in the BV oxidation of the series of cyclic ketones [19]. Quite interestingly, the outcome showed that in the absence of catalyst no lactones were detected. Kawabata *et al.* [20] described the application of iron containing MCM-41 catalysts with tetrahedrally coordinated Fe species, which demonstrated both the high conversion of 2-adamantanone and the high yield to lactone. After reaction, a catalyst was recovered from the

reaction mixture by filtration for the repeated oxidations of cycloketone without any observable loss in activity or selectivity.

Despite the rich literature on the use of mesoporous catalysts in the BV oxidation in Mukaiyama conditions, until now Ti-containing BEA zeolites have never been studied. This urged us to study on the catalytic behavior of siliceous Ti-containing BEA zeolites with Ti atoms incorporated in the framework as tetrahedrally coordinated Ti species. Ti_xSiBEA zeolite series was prepared and applied in the liquid-phase BV oxidation of cyclohexanone to ε-caprolactone in the oxygen-aldehyde system.

It is generally accepted that framework tetrahedral Ti(IV) ions in silicalite and BEA zeolite are the active sites of selective oxidation of cyclic and linear alkenes [21,22]. As it was previously shown [23-28], the incorporation of transition metal ions into the framework of BEA zeolite is strongly favored when, in the first step, BEA is dealuminated by nitric acid solution treatment. Then, in the second step, the incorporation of transition metal ions into zeolite matrix results from the reaction between the cationic metal species of the precursor solution and the SiO-H groups of vacant T-atom sites created by the dealumination of BEA zeolite. The post-synthesis method applied earlier for the solid-liquid interface and vanadium, cobalt, iron and copper [23-28] has been extended to the solid-gas interface and titanium, with $TiCl_4$ vapor as the precursor [29,30].

The aim of the present work was to show the effect of the nature and environment of titanium present in Ti_xSiBEA zeolites on the liquid-phase Baeyer-Villiger oxidation of cyclohexanone to ε-caprolactone in the oxygen-aldehyde system (Mukaiyama regime) (Fig. 1).

- Figure 1-

Such method of ε-caprolactone synthesis offers the application of milder reaction conditions, more compatible with the idea of sustainable development. The state of titanium in the Ti_xSiBEA zeolite series, where x = 0.8, 1.1, 2.0, 2.6, 4.3 Ti wt %, was characterized by NMR, DR UV-vis and XPS techniques. Catalytic properties of Ti_xSiBEA zeolites were compared with that of parent SiBEA zeolite.

Experimental Section

Materials

A tetraethylammonium BEA (TEABEA) zeolite provided by SINOPEC Research Institute of Petroleum Processing (RIPP), Beijing, China was calcined (air, 15 h, 823 K) to obtain an organic-free HAlBEA (Si/Al = 11). To obtain a dealuminated organic-free BEA, initial TEABEA zeolite was treated in a 13 mol L^{-1} HNO_3 solution for 4 h at 353 K under stirring in an ordinary laboratory glass beaker covered with a laboratory glass slide limiting the rapid evaporation of nitric acid solutions. The resulting SiBEA (Si/Al = 1000) with vacant T-atom sites was recovered by centrifugation, washed with distilled water, and dried overnight at 353 K in air. To incorporate titanium ions into siliceous BEA zeolite, 2 g of SiBEA were treated in a fixed-bed reactor at 423 K for 3 days in flowing oxygen. Then, temperature was increased to 573 K and the solid was subjected, for 0.5, 1, 4, 5 and 10 h, to a nitrogen flow (100 cm^3 min^{-1}) through a saturator containing liquid $TiCl_4$ (Aldrich, purity 99.9 %) at 266 K. The $TiCl_4$ vapour pressure in the saturator was 200 Pa and the volume to volume (v/v) ratio of $TiCl_4$ and N_2 was 0.2 %. The solid was treated under $TiCl_4$-containing nitrogen flow at 573 K for 2 h, cooled to room temperature and exposed to moist air for 12 h, dried in air at 353 K for 12 h and finally calcined in flowing dry air at 723 K for 4 h.

Methods

An inductively coupled plasma optical emission (ICP-OES Quantima Sequential) spectrometer from GBC was used to specify the Al, Si, Ti content in the zeolite's samples. Chemical analysis of these samples was performed at the Service Central d'Analyse, CNRS, Vernaison, France.

The XRD measurements were carried out on a PANalytical X'Pert Pro diffractometer using Cu K_α radiation (λ = 154.05 pm) in 2θ range of 5 - 90°.

X-ray fluorescence (XRF) analysis was performed using Skayray EDX 3600H spectrometer equipped with the tungsten lamp and having analytical range from 1 ppm to 99.99 % and spectrometer sensitivity 0.05 % wt. Prior to the measurement, the reaction mixtures containing the solid catalyst suspended in the liquid phase were centrifuged and solid material was separated from the solution. For analysis the resultant solutions were placed inside the XRF cell.

The FTIR spectra of studied samples were recorded on Bruker Vector 22 spectrometer equipped with DTGS detector with resolution 2.0 cm^{-1} and number of scans amounting to 128. Prior to the measurement, the samples (about 20 mg) were pressed at ~ 1 ton cm^{-2} into thin wafers of approximately 10 mg cm^{-2} by using a hydraulic press and next placed inside the IR cell. The wafers were calcined at 723 K for 3 h in O_2 (0.750 Pa) and then outgassed at 573 K (10^{-3} Pa) for 1 h. After that, the spectra were registered in the range characteristic for OH groups. To analyse the acidity of HAlBEA and SiBEA supports as well as Ti_xSiBEA zeolite catalysts prepared in such a way, the wafers were contacted with gaseous pyridine (0.0075 Pa) via a separate cell contacting liquid pyridine at room temperature. After the desorption of pyridine at 423 K for 1 h the FTIR spectra were recorded at room temperature in the range of 4000 - 400 cm^{-}

[1]. Next, the spectra were registered in the range of 1700 - 1400 cm^{-1} where the bands related to the pyridine chemisorbed on Brønsted or Lewis acid sites occur.

Solid state magic angle spinning nuclear magnetic resonance (MAS NMR) experiments were performed on a Bruker AVANCE500 spectrometer at 11.7 T in 4 mm zirconia rotors spinning at 14 kHz. The resonance frequency of ^{1}H and ^{27}Al were 500.16 and 130.33 MHz, respectively. Chemical shifts, δ, were reported relative to tetramethylsilane (TMS) and aqueous $Al(NO_3)_3$ 1 N solution. ^{1}H MAS NMR spectra were performed with a 90° pulse duration of 2 μs and a recycle delay of 5 s and 16 accumulations. ^{27}Al MAS NMR spectra were recorded by small-flip-angle technique with a pulse of 0.9 μs (π/8), 0.5 s for the recycle delay and 2048 accumulations. ^{29}Si MAS NMR spectra as well as ^{1}H - ^{29}Si MAS NMR of as prepared samples, transferred at ambient atmosphere into 7 mm zirconia rotors, were performed at 79.5 MHz. Chemical shifts of silicon were measured by reference to TMS. ^{29}Si MAS NMR spectra were obtained with 4 kHz spinning speed, 2.5 ms excitation pulse and 10 s recycle delay. Polydimethylsilane was used for setting the Hartmann-Hahn condition. The proton π/2 pulse duration, the contact time and recycle delay were 6.8 ms, 5 ms and 5 s respectively.

Diffuse reflectance UV−Vis spectra were recorded in ambient atmosphere on a Cary 5000 Varian instrument with polytetrafluoroethylene as reference.

The X-ray Photoelectron Spectroscopy (XPS) measurements were carried out with a hemispherical analyzer (SES R4000, Gammadata Scienta). The unmonochromatized Mg Kα (1253.6 eV) X-ray source with the anode operating at 12 kV and 15 mA current emission was applied to generate core excitation. The energy resolution of the system, measured as a full width at half maximum (FWHM) for Ag $3d_{5/2}$ excitation line, was 0.9 eV (pass energy 100 eV). The spectrometer was calibrated according to ISO 15472:2001. The base pressure in the analysis

chamber was about 5×10^{-9} mbar during the experiment. The powder samples were pressed into indium foil and mounted on a dedicated holder. All spectra were collected at pass energy of 100 eV (with 25 meV step) except survey scans which were collected at pass energy of 200 eV (with 0.25 eV step). The area of sample analysis was about 3 mm^2. Intensities were estimated by calculating the integral of each peak (CasaXPS 2.3.19), after subtraction of the Shirley-type background, and fitting the experimental curve with a combination of Gaussian and Lorentzian lines of variable proportions (70:30). The Ti 2p core excitations were deconvoluted with a relative intensity ratio of $2p_{3/2}$ and $2p_{1/2}$ lines fixed to 2:1. The samples were weak conductive, thus all binding energy (BE) values were charge-corrected to the carbon C 1s excitation which set at 285.0 eV.

Concentration of perbenzoic acid was determined using iodometric titration. Portions of reaction mixture were analyzed after 1, 2, 3, 4 and 5 hours of BV oxidation. A sample of known amount of reaction mixture was mixed with 50 mL 2 M H_2SO_4 and 10 mL of saturated KI solution. The resultant mixture was titrated with 0.1 M sodium thiosulphate solution until the color turned into pale yellow. At this point 2 ml of starch was added as an indicator and the dark blue mixture was titrated until the color disappeared completely.

Catalytic measurements

The liquid-phase Baeyer-Villiger oxidation of cyclohexanone with molecular oxygen was performed in a thermostated home-made glass reactor at 313 K for 5 h at atmospheric pressure. In a typical experiment, 0.01 mM of a catalyst (catalyst mass ranged from 0.0598g for $Ti_{0.8}$SiBEA to 0.0111g for $Ti_{4.3}$SiBEA), 4.6 mmol of cyclohexanone, and 14 mmol of benzaldehyde were dissolved in acetonitrile. During the reaction, the concentration of oxygen was kept constant with aid of the valves system controlling the level of oxygen in the reaction

mixture (Figure S1). The conversion of substrate and the percentage yield of ε-caprolactone were determined using gas chromatograph (Agilent Technologies 6890N) equipped with an Innowax (30 m) column. The percentage yield of oxygenates was determined in the presence of chlorobenzene as internal standard.

Results and Discussion

The structural characterisation

The Ti_xSiBEA samples prepared by two-step post-synthesis method are white in colour and correspond to x = 0.8, 1.1, 2.0, 2.6 and 4.3 Ti wt % as determined by chemical analysis (ICP-OES method).

XRD patterns of SiBEA and Ti_xSiBEA are presented in Figure 2. They are typical of BEA zeolite. The characteristic reflections for Beta zeolite materials at around 2θ of 7.5 and 22.4° are observed for all tested systems. The XRD results show that the removal of aluminium from zeolite framework followed by the introduction of titanium does not affect its crystalline structure, in line with earlier reports [31,32]. The crystallinity of zeolite is preserved after dealumination and no evidence of extra lattice crystalline compounds or long-range amorphization of the zeolite structure are observed.

The two-step post-synthesis procedure used for samples preparation did not significantly change the textural properties of zeolites upon acid treatment and the introduction of titanium into SiBEA support. They also present quite large specific surface area (> 450 m^2 g^{-1}) in line with the prevailing porosity usually reported for the BEA topology: 600 m^2 g^{-1} for HAlBEA, 610 m^2 g^{-1} for SiBEA, 590 m^2 g^{-1} for $Ti_{1.1}$SiBEA, 570 m^2 g^{-1} for $Ti_{2.0}$SiBEA and 460 m^2 g^{-1} for

$Ti_{4.3}$SiBEA samples. It should be noted, however, that the introduction of Ti consistently decreases the surface area, in particular for $Ti_{4.3}$SiBEA sample.

The surface composition of Ti_xSiBEA zeolites is presented in Table S1. The calculations have been performed on the assumption that samples are composed of pure and uniform SiO_2 with density equal to 2.18 g cm^{-3}. Results in Table S1 confirm that surface concentration of Ti increases with the increase of number of titanium cations incorporated into BEA zeolite.

- Figure 2 -

The evidence of Al removal and Ti incorporation upon two-step post-synthesis preparation

The FTIR spectrum of HAlBEA exhibits five IR bands (Fig. 3) respectively attributed to AlO-H groups (3778 and 3661 cm^{-1}), bridging acidic hydroxyls Si-O(H)-Al (3607 cm^{-1}), isolated external SiO-H groups (with a narrow band at 3740 cm^{-1}) and hydrogen bonded SiO-H groups (a broad band at 3523 cm^{-1}) [33-35]. Upon dealumination, the three bands related to AlO-H and Si-O(H)-Al groups disappeared suggesting that aluminium is removed. The appearance of IR bands related to isolated internal silanol groups at 3736 cm^{-1} and an intense broad band of H-bonded SiO-H groups at 3523 cm^{-1} for SiBEA reveal the creation of vacant T-atom sites associated with silanol groups upon removal of framework aluminium. The intensity of the band at 3523 cm^{-1}, observed for the Ti_xSiBEA samples, decreased comparing to SiBEA, confirming that $TiCl_4$ vapour has reacted with hydrogen bonded silanol groups present in vacant T-atom sites and Ti ions are incorporated into zeolite framework.

- Figure 3 -

^{27}Al MAS NMR spectra of HAlBEA, SiBEA and Ti_xSiBEA samples are shown in Fig. 4. HAlBEA shows two main peaks at around 52.7 and -2.0 ppm, first one assigned to tetrahedral

Al_{Td} and second one to octahedral Al_{Oh}. After dealumination, the intensity of the signal at 52.7 ppm corresponding to Al_{Td} decreases drastically (Fig. 4). Moreover, one can observe in SiBEA sample very sharp signal at -0.1 ppm which is probably related to the octahedral Al species formed as a result of coordination of trace amounts of Al_{Td} present in SiBEA with two H_2O molecules [36-40].

After incorporation of Ti ions into SiBEA zeolite only characteristic Al_{Td} band at 53.3 ppm is present in the spectra of all Ti_xSiBEA samples (Fig. 4).

- Figure 4 -

The incorporation of Ti ions into SiBEA matrix has also been confirmed by ^{29}Si MAS NMR spectra (Fig. 5) and ^{1}H - ^{29}Si cross polarisation (CP) MAS NMR spectra (Fig. 6). The ^{29}Si MAS NMR spectrum of SiBEA shows three peaks at -101.7, -110.5 and –114.3 ppm. The peak at -101.7 ppm is assigned to Si atoms in $Si(OH)(OSi)_3$ environment as revealed by the strong increase of intensity of the peak at -101.8 ppm when CP is applied (Fig. 6), the technique which preferentially enhances the signal of ^{29}Si nuclei close to protons as in the case of $Si(OH)(OSi)_3$ site.

- Figure 5 -

In the CP spectrum of Ti_xSiBEA, a weak peak at -92 ppm can also be seen evidencing the presence of small amounts of Si atoms in $Si(OH)_2(OSi)_2$ environment (Fig. 6). The peak at -110.5 ppm with a shoulder at around -114.3 ppm results from the framework Si atoms in $Si(SiO)_4$ environment, located at different crystallographic sites, in line with the earlier reports on BEA zeolite [29,41]. After the incorporation of Ti cations into SiBEA zeolite the intensity of the band at -101.7 ppm assigned to Si atoms in a $Si(OH)(OSi)_3$ environment decreased (Fig. 5)

proving the reaction of these groups with Ti cations (decomposition and integration are presented in supplementary data Figure S2 and Table S2).

- Figure 6 -

In the ^{1}H MAS NMR spectrum of HAlBEA (Fig. 7), two main peaks at 1.8 and 4.9 ppm are observed due to the protons of isolated and H-bonded silanol groups, respectively, in line with earlier data on BEA [42,43], MFI [44,45], silicalite [46] and silica [47]. Slightly shifted values are found for the same groups of protons in SiBEA at 1.3 and 5.3 ppm, respectively. A small peak at 3.2 ppm, observed for SiBEA zeolite, is probably due to the presence of protons of H-bonded SiO-H groups located in the different type of crystallographic sites, similar to those observed in silica [47].

- Figure 7 -

The disappearance of the peak at 3.2 ppm and shift of the peaks from 1.3 and 5.3 ppm to 1.2 and 4.6 ppm, respectively, upon incorporation of Ti atoms into SiBEA (Fig. 7) evidences the reaction of $TiCl_4$ vapour with H-bonded and isolated SiO-H groups, as reported earlier for TiSiBEA zeolite [29].

The NMR spectra of Ti-containing SiBEA still exhibit the peak visible at 4.5 - 4.8 ppm assigned to H-bonded SiO-H groups but with lower intensity than the one observed for SiBEA support. Concluding, the above demonstrates that silanol groups are consumed upon reaction with $TiCl_4$ vapor. The small peaks at 1.2 and 0.9 ppm (Fig. 7) are probably due to very low content of protons of isolated SiO-H groups present in Ti_xSiBEA zeolites. Moreover, another small peak at 3.7 ppm observed for $Ti_{1.1}$SiBEA, $Ti_{2.0}$SiBEA, $Ti_{2.6}$SiBEA and $Ti_{4.3}$SiBEA is probably due to the protons of particular SiO-H present in environment of Ti(IV) species.

Titanium state in Ti_xSiBEA zeolites

The DR UV-vis spectra of Ti_xSiBEA (Fig. 8) exhibit the large band between 220 and 350 nm assigned to oxygen-tetrahedral Ti(IV) and oxygen-octahedral Ti(IV) ligand to metal charge transfer (LMCT) transitions, as reported earlier for TiBEA and TiMCM-41 materials [29,48-52]. The band visible at around 330 nm is generally associated with the presence of octahedral Ti(IV). In contrast, the band at around 230 nm is associated with the presence of tetrahedral Ti(IV) and could be assigned to oxygen to tetrahedral Ti(IV) charge transfer (CT) transition, in line with earlier reports [29,48] and confirms the incorporation of Ti atoms into the SiBEA framework**.**

- Figure 8 -

The X-ray photoelectron spectra of Ti_xSiBEA samples, have been analyzed numerically in the BE regions of Si 2p, Al 2p, O 1s, C 1s, and Ti 2p. All Si 2p spectra are described by a single doublet with the spin-orbit splitting of 0.61 eV (Fig. S3). Si $2p_{3/2}$ BE values of 104.1-104.3 eV are related to the presence of tetrahedral Si(IV) [53-55], however, they are slightly larger than reported earlier for BEA, MFI and MOR zeolites with other cations [56-60]. Some traces (<0.1% at.) of aluminum were found in the Al 2p high resolution spectra of $Ti_{1.1}SiBEA$ and $Ti_{2.0}SiBEA$ (Fig. S4), which suggests that the dealumination of HAlBEA into SiBEA was not completed. The binding energy of Al $2p_{3/2}$ peaks are close to 75.0 eV proving the presence of Al^{3+} (Al_2O_3 BE = 74.9 eV [61]).

The O 1s peaks can be well fitted by three components (Fig. S5): (i) a main peak (>80% of total spectrum area) located close to 533.5 eV and assigned to oxygen in the zeolite framework (Si-O-Si bonds) [62-64]; (ii) a low-BE peak close to 531.5 eV due to Ti-O-Si bonds [65-68]; (iii) a peak at BE higher than 534.3 eV assigned to adsorbed water, OH groups and/or oxygen of organic contaminants. However, the fact that the low-BE component at 530.4 eV (which could be ascribed to the oxygen in TiO_2 anatase [69]) was not found in our samples is of no

significance. The shift towards higher BE of Ti-O-Si peak with respect to that of pure TiO_2 can be explained by the decrease of the coordination number of titanium and shortening of the Ti-O bond which increase the interatomic potentials. The silica lattice may maintain high electron densities on the oxygen atoms since the Si atoms are more electronegative and less polarizable than the Ti atoms. The presence of Ti-O bond in the zeolite indicates that Ti and Si ions are chemically bound to each other via Ti-O-Si bridges. This also supports the suggestion that titanium is monoatomically dispersed in our samples.

- Figure 9 -

The C 1s core lines generally consist of four peaks: two most intense components at 285.0 eV (organic contaminants) and 286.2–286.5 eV (C–O groups) covering more than 90 % of total spectrum area, and two weak ones with BE >289.1 eV (O-C=O groups) and <282.0 eV (carbides) (Fig. S6).

The XPS spectra of Ti 2p obtained for all Ti_xSiBEA zeolite catalysts are presented in Fig. 9. Due to the spin-orbit coupling, the Ti 2p core lines are splitted into well separated doublet structures (Ti $2p_{3/2}$ and $2p_{1/2}$). The main parameters of the fitted components are presented in Table 1. The deconvoluted spectra show two components with very high values of Ti 2p binding energy. Taking into account, that the following Ti $2p_{3/2}$ values are reported: 455.3 eV for Ti(II) in TiO, 457.1 eV for Ti(III) in Ti_2O_3 and 458.7 eV for Ti(IV) in TiO_2 one can identify both components as coming from the presence of Ti(IV) species only [70 and references therein]. Due to unmonochromatized Mg Kα X-ray source, an additional low-BE component coming from higher components of characteristic X-rays ($K\alpha_3$ and $K\alpha_4$, marked as Kα sat in Fig. 9) is present in all spectra.

- Table 1 -

One can find the unusually high-BE component with Ti $2p_{3/2}$ binding energy in the range of 460.1-460.6 eV (Table 1). The position of this high-BE component is shifted more than 1 eV toward higher energy with respect to the one found in TiO_2. It is worth mentioning that many metal cations (e.g. Fe, Cr, Cu) located in zeolites also exhibit higher BE comparing with their BE in oxides [2,28,71]. This can be affected by the degree of cations dispersion (even occurrence of highly isolated species) as well as by the nature of their interactions with the zeolite matrix in which they are embedded. On the basis of previous assignments for TiO_2-SiO_2 glasses [34,72,73] and titanosilicate molecular sieves TS [74], one can attribute this high-BE component to the tetrahedrally coordinated intra-framework titanium. Such isolated tetrahedral Ti(IV) species embedded into the zeolite matrix are bonded to the silica network by Ti-O-Si bridges. With titanium loading increase, the position of this component does not change significantly, but a second component starts to grow. This component with little lower Ti $2p_{3/2}$ binding energy of 458.2-459.9 eV has also BE different from the one observed for titanium in bulky TiO_2 anatase, indicating that titanium is present in various environments. It can be attributed to the Ti atoms that are not completely isolated but can exist as extra-framework Ti-O-Ti species in Ti-rich nanodomains/clusters, that grow progressively with Ti content [75]. It is confirmed by a significant increase of low-BE component area and its BE shift towards higher energy with the Ti loading growth (Fig. 9). The absence of a bulk titania-like phase is in line with our interpretation of O 1s XPS spectra.

Some additional information, helpful in the full characterization of XPS spectra, can be achieved from the distance between two peaks in the doublet (spin-orbit splitting Δ, see Table 1). The spin-orbit splitting of low–BE Ti 2p doublets (Δ_A) is in the range of 4.7-5.0 eV and is independent of the titanium loading, in contrast to high-BE ones (Δ_B) which achieve the values

of 5.0-5.9 eV and strongly increase with the rise of the Ti content. It is relatively rare to find Ti 2p spin-orbit splitting values in the literature besides most common separation of 5.75 eV in TiO_2 [76]. However, some other values are reported by Biesinger *et al.* [70] who state that Ti 2p splitting decreases with the increase of Ti oxidation state. Relatively low values of Ti 2p splitting obtained in our analysis confirm that only Ti(IV) species are present in the Ti_xSiBEA samples and the formation of titanium bulk phases is not observed.

Acidic properties of catalytic systems

To determine the nature and strength of acidic centres in HAlBEA, SiBEA and Ti_xSiBEA zeolites the adsorption of pyridine as probe molecules has been performed. Fig. 10 shows the FTIR spectra of HAlBEA, SiBEA, $Ti_{0.8}$SiBEA, $Ti_{1.1}$SiBEA, $Ti_{2.0}$SiBEA, $Ti_{2.6}$SiBEA and $Ti_{4.3}$SiBEA after adsorption of pyridine at room temperature and followed desorption at 423 K.

For HAlBEA very intense bands at 1636, 1622, 1608, 1545, 1490 and 1453 cm^{-1} are observed. The bands typical of pyridinium cations are seen at 1636 and 1545 cm^{-1}, indicating the presence of strong Brønsted acid centres, probably related to the acidic proton of Al-O(H)-Si groups, in line with earlier data obtained for BEA zeolites [35,77]. The bands at 1622 and 1453 cm^{-1} correspond to the pyridine interacting with strong Lewis acid centres (Al^{3+}). The band at 1490 cm^{-1} corresponds to the pyridine interacting with Brønsted and Lewis acid centres while the one at 1608 cm^{-1} corresponds to the pyridine coordinated to moderate Lewis acid centres (Al^{3+}) [35,77]. Moreover, the small band at 1575 cm^{-1} originates from the physisorbed pyridine.

For SiBEA only traces of Brønsted and Lewis acid centres (see band at 1490 cm^{1}) are present as shown in Figure 10 and Table 2. After incorporation of Ti ions into the framework of Ti_xSiBEA zeolite a very small amount of Brønsted and Lewis acid centres appears as shown by the stepwise increase of 1636, 1622, 1608, 1546, 1490 and 1445 cm^{-1} bands intensity with the Ti

content growth (Fig. 10). The formation of Brønsted and Lewis acid centres in Ti_xSiBEA zeolite is probably related to the formation of $Ti(III)(OSi)_3$-O(H)-Si species. Brønsted acid properties appear due to the presence of acidic proton of bridged OH group while Lewis acid properties are generated in the presence of Ti(III). Similar species, $Fe(III)(OSi)_3$-O(H)-Si and $Cr(III)(OSi)_3$-O(H)-Si observed for Fe_xSiBEA and Cr_xSiBEA zeolites, respectively, were already postulated [71,78,79]. The $Ti(III)(OSi)_3$-O(H)-Si species could be formed simultaneously with $Ti(IV)(OSi)_4$ species, the latter being the main species in Ti_xSiBEA. The formation of Brønsted and Lewis acid centres in Ti_xSiBEA has previously been observed in earlier works of Dzwigaj et al. [29,30]. As shown in Table 2, the number of Brønsted and Lewis acid centres [80] increases with the rise of titanium incorporated into the SiBEA up to 2.6 wt %. For the highest Ti content ($Ti_{4.3}SiBEA$), the number of Brønsted and Lewis acid centres decreases (Table 2). Such decrease is probably related to the incorporation of higher number of Ti cations into the extra-framework positions of $Ti_{4.3}SiBEA$ as octahedral Ti(IV) species which block some part of framework tetrahedral $Ti(III)(OSi)_3$-O(H)-Si sites.

- Figure 10 –

- Table 2 -

Catalytic activity

The effect of the titanium state present in the Ti_xSiBEA zeolites on their catalytic activity in the BV oxidation of cyclohexanone to ε-caprolactone under the Mukaiyama regime has been studied. The results shown in Table 3 demonstrate that all the examined zeolite catalysts were active in the studied reaction and their catalytic behavior was changing together with the titanium content and its local environment in zeolite framework [81].

- Table 3 -

SiBEA zeolite displays the lowest catalytic activity among all the studied catalysts. Its low catalytic activity is linked with the lack of catalytically active Ti atoms in framework positions. However, observed non-zero catalytic activity is probably related to the traces of Al(III) atoms still present in SiBEA (see Figure 10, Table 2) after dealumination of TEABEA zeolite. In the presence of aluminium cations, the formation of Al(III)$(OSi)_3$-O(H)-Si species, possessing both the Brønsted and the Lewis acid properties, could be postulated due to the presence of acid protons (bridged OH groups) and Al^{3+}, respectively. The presence of the latter allows cyclohexanone to be activated on the catalyst Lewis metal center. Recently, Corma *et al.* [82] reported that Lewis acidity could be formed in SnBEA zeolite when framework tin atoms are coordinated by three silyloxy groups and one hydroxy group. Moreover, in zeolite materials almost always iron impurities in the form of tetrahedral Fe(III)$(OSi)_3$-O(H)-Si species are present and even treatment with nitric acid does not remove all of them from the framework, as it was already reported in our previous work [83]. Traces of these species, having acid and redox properties could facilitate the oxidation of aldehyde to peracid as well as activation of cyclohexanone thus, playing the role of bi-functional catalyst in the oxidation of cyclohexanone to ε-caprolactone (see Table 3).

With the increase of titanium content in the Ti_xSiBEA catalysts up to x = 2.0 wt %, both the conversion of substrate and the yield to ε-caprolactone gradually rise. $Ti_{2.0}$SiBEA catalyst which is characterized by the maximum number of isolated tetrahedral Ti(IV) sites revealed the conversion of 77.4 % and the selectivity to lactone reached 98.6 %. However, starting from $Ti_{2.6}$SiBEA zeolite a gradual decline of catalytic activity can be observed. Furthermore, $Ti_{2.0}$SiBEA and $Ti_{2.6}$SiBEA catalysts were recovered from the reaction mixture by filtration and they were reused twice without significant loss of catalytic activity (see Table 3). The slight

decrease in TON for $Ti_{2.6}$SiBEA can be attributed to the handling of the catalyst. Catalytic results obtained for recovered samples indicate that Ti_xSiBEA zeolites are stable and regenerable catalysts in BV oxidation.

It is widely acknowledged that for the Mukaiyama system sacrificial aldehyde with molecular oxygen added into the reaction mixture enable the transformation of cyclic ketones into their corresponding lactones through the *in situ* peracid formation. To establish the amount of peracid formed during the reaction course the iodometric analysis for $Ti_{2.0}$SiBEA was performed. The remaining perbenzoic acid was reduced with iodine which was next titrated with thiosulfate. The results of iodometric titrations presented in Figure 11 demonstrate the variation of the perbenzoic acid concentration as a function of reaction time. The concentration of perbenzoic acid increases fast during the first two hours, than slows down until the maximum, reached after the fourth hour of the reaction. As the reaction proceeds further the perbenzoic acid concentration drops.

- Figure 11 -

Basing on the results of the present study as well as literature data [13,84], the catalytic investigations revealed that the active catalyst of the studied BV oxidation reaction is the bi-functional catalyst, which catalyzes the different reaction stages. It is generally accepted that BV oxidation in the Mukaiyama conditions proceeds efficiently via free radical chain mechanism [12,14]. The redox function of the catalyst is needed for the oxidation of aldehyde to peracid. The reaction starts with the abstraction of hydrogen from aldehyde to produce acyl radical $RCO^{\bullet}$. It is very probable that in the presence of Ti_xSiBEA as catalyst, hydrogen is abstracted by titanium with its highest oxidation state and the resulting acyl radical reacts further with O_2 to form acylperoxy radical $RCOOO^{\bullet}$. The newly formed acylperoxy radical abstracts hydrogen from the next aldehyde molecule to afford *in situ* formation of peracid RCOOOH.

The Lewis acid function is necessary for the activation of ketone carbonyl group while the decomposition of Criegee adduct to ε-caprolactone could take place on the Brønsted acid sites. Activation of carbonyl group, occuring via the coordination of cyclohexanone molecule to the Lewis acid center, was confirmed by *in situ* IR spectroscopy [84]. The nucleophilic attack of the peracid onto the more electrophilic carbon atom from activated carbonyl group results in the formation of the Criegee complex [31]. The formation of the latter one was recognized by the isotopic studies [85].

The key objective of the preparation of the series of Ti_xSiBEA catalysts for the application in the BV oxidation of cyclohexanone with molecular oxygen and aldehyde as oxidant was formation of tetrahedrally coordinated titanium (IV) species (Ti(IV)$(OSi)_4$) in the framework positions. Such Ti centres are known to be able to activate dioxygen by the formation of peroxo complexes [86], therefore their presence is essential for oxidation of the sacrificial aldehyde to peracid. Moreover, as it was already postulated, the presence of Ti(III)$(OSi)_3$-O(H)-Si, Al(III)$(OSi)_3$-O(H)-Si or Fe(III)$(OSi)_3$-O(H)-Si species which possess Brønsted acid sites due to the existence of acid protons of bridged OH groups and Lewis acid sites attributed to Ti^{3+}, Al^{3+} or Fe^{3+} cations allows us to obtain bi-functional system capable to oxidize cyclohexanone to ε-caprolactone.

Table 1 demonstrates that the stepwise increase of the titanium content generates, besides tetrahedrally coordinated Ti(IV) species such as Ti(IV)$(OSi)_4$, octahedrally coordinated titanium Ti(IV) species like $(H_2O)_2$(Ti(IV)$(OSi)_4$ in the framework and extra-framework positions. The rising number of the octahedrally coordinated titanium species might reduce the catalytic activity as it is observed for $Ti_{2.6}$SiBEA through the limited access of reagents to the framework tetrahedral Ti(IV)$(OSi)_4$. Enhanced decrease of catalytic activity observed in the case of

$Ti_{4.3}$SiBEA probably results from the increased quantity of octahedral $(H_2O)_2(Ti(IV)(OSi)_4$ species that could block the accessibility of framework tetrahedral $Ti(IV)(OSi)_4$ and $Ti(III)(OSi)_3$-O(H)-Si centers, resulting in the decrease of cyclohexanone conversion. Figure 8 confirms the substantial growth of octahedrally coordinated titanium species for $Ti_{2.6}$SiBEA and $Ti_{4.3}$SiBEA zeolites.

Table 2 demonstrates that the number of Brønsted acid sites gradually increases with the growth of Ti content in Beta zeolite. This cannot be explained only by the presence of aluminium traces detected by the XPS spectroscopy or iron traces reported in our previous paper [82]. Therefore, an alternative source of Brønsted acidity must exist. The possible elucidation of the Brønsted acidity increase could be the incorporation of minor number of titanium sites, in the form of $Ti(III)(OSi)_3$-O(H)-Si species, into zeolite framework positions. These species play both, the role of Brønsted acid sites associated with the presence of acidic bridged OH groups and the function of Lewis acid centers due to the presence of Ti^{3+} cations. Therefore, as it was shown in Table 2, the increase of the Brønsted acidity is accompanied by the rise of Lewis acidity as a result of the stepwise Ti content growth.

Another factor, important for heterogeneously catalyzed liquid phase reactions, that might influence the catalytic activity of the series of Ti_xSiBEA zeolites in the studied reaction concerns leaching of the titanium cations from BEA zeolite framework into the liquid medium. Leaching of catalyst components into the liquid phase is an important issue regarding its irreversibility, threatening the sustainability of the process and finally leading to catalyst deactivation [87]. To check the possibility of leaching of the titanium ions from Ti_xSiBEA solids the XRF analysis of the liquid phase, received after solid catalyst separation, was performed. XRF analysis revealed

the presence of no titanium cations in the reaction mixtures taken after the termination of BV oxidation.

Conclusions

Ti_xSiBEA zeolites (x = 0.8, 1.1, 2.0, 2.6 and 4.3 Ti wt %) are prepared by a two-step post-synthesis method involving (i) dealumination of TEABEA zeolite by nitric acid leading to nests of SiO-H groups in vacant T-atom sites and (ii) incorporation of Ti into SiBEA zeolite by reacting $TiCl_4$ vapour with those silanol groups.

The incorporation of Ti cations into the SiBEA framework is evidenced by FTIR, ^{29}Si MAS NMR, ^{1}H - ^{29}Si CP MAS NMR and ^{1}H MAS NMR.

DR UV-vis and XPS investigations show that, for low titanium content, mainly framework tetrahedral Ti(IV) species are present in Ti_xSiBEA zeolites. For titanium content higher than 2.6 wt %, apart from the framework tetrahedral Ti(IV) species, also octahedral Ti(IV) species are formed.

The acidity is a key factor for efficient transformation of cyclohexanone to ε-caprolactone in the BV oxidation depending on the titanium oxidation state and environment. Brønsted acid properties appear due to the presence of acidic protons of bridged OH groups while Lewis acid properties are generated due to the presence of Ti(III) species. The Ti(III)$(OSi)_3$-O(H)-Si are formed simultaneously with Ti(IV)$(OSi)_4$, the latter being the main species in Ti_xSiBEA. The number of Brønsted and Lewis acid centres increases with the rise of titanium content in the Ti_xSiBEA up to 2.6 wt %.

For $Ti_{4.3}$SiBEA zeolite with the highest Ti content, the number of Brønsted and Lewis acid centres decreases. Such decrease is related to the incorporation of higher number of Ti cations into the extra-framework positions of $Ti_{4.3}$SiBEA as octahedral Ti(IV) which block the part of framework tetrahedral Ti(IV)$(OSi)_4$ and Ti(III)$(OSi)_3$-O(H)-Si centres.

Among all of the studied Ti_xSiBEA catalysts, the highest catalytic activity is observed for $Ti_{2.0}$SiBEA zeolite. The Ti_xSiBEA zeolites applied in the liquid-phase Baeyer-Villiger oxidation of cyclohexanone to ε-caprolactone in the oxygen-aldehyde system as catalysts are bi-functional, possessing both the acidic and redox properties, catalyzing different reaction stages. $Ti_{2.0}$SiBEA and $Ti_{2.6}$SiBEA catalysts were recycled twice without a significant loss of catalytic activity.

The Baeyer-Villiger oxidation mechanism is discussed with respect to different nature and environment of titanium in SiBEA zeolite determining its redox and acid function.

ASSOCIATED CONTENT

Supporting Information Available. Surface composition of Ti_xSiBEA catalysts is included.

References

[1] G. Strukul, Transition Metal Catalysis in the Baeyer–Villiger Oxidation of Ketones, Angew. Chem. Int. Edit. 37 (1998) 1199-1209. DOI:10.1002/ (SICI)1521-3773(19980518)37:9<1198: AID-ANIE1198>3.0.CO;2-Y.

[2] L. Balbinot, U. Schuchardt, C. Vera, J. Sepúlveda, Oxidation of cyclohexanol to epsilon-caprolactone with aqueous hydrogen peroxide on $H_3PW_{12}O_{40}$ and $Cs_{2.5}H_{0.5}PW_{12}O_{40}$, Catal. Commun. 9 (2008) 1878-1881. DOI:10.1016/j.catcom.2008.03.006.

[3] G. J. ten Brink, I. W. C. E. Arends, R. A. Sheldon, The Baeyer-Villiger reaction: new

developments toward greener procedures, Chem. Rev. 104 (2004) 4105-4123. DOI: 10.1021/cr0300111.

[4] S. E. Jacobson, R. Tang, F. Mares, Oxidation of cyclic ketones by hydrogen peroxide catalysed by Group 6 metal peroxo complexes, J. Chem. Soc. Chem. Comm. 20 (1978) 888-889. DOI:10.1039/C39780000888.

[5] E. C. B. A. Alegria, L. M. D. R. S. Martins, M. V. Kirillova, A. J. L. Pombeiro, Baeyer–Villiger oxidation of ketones catalysed by rhenium complexes bearing N- or oxo-ligands, Appl. Catal. A 443-444 (2012) 27-32. DOI:10.1016/j.apcata.2012.07.007.

[6] Q. Ma, J. R. Zhao, W. Z. Xing, X. H. Peng, Baeyer-Viiliger Oxidation of Cyclic Ketones Using Aqueous Hydrogen Peroxide Catalyzed by Heteropolyacids in Solvent-free System, J.Adv. Oxid. Technol. 17 (2014) 212-216. DOI:10.1515/jaots-2014-0206.

[7] Z. Yang, X. Xu, T. Li, N. Zhang, X. Zhao, W. Chen, X. Liang, X. He, H. Ma, Preparation and Catalytic Property of Multi-walled Carbon Nanotubes Supported Keggin-Typed Tungstosilicic Acid for the Baeyer–Villiger Oxidation of Ketones, Catal. Lett. 145 (2015) 1955-1960. DOI:10.1007/s10562-015-1601-9.

[8] A. Corma, L. T. Nemeth, M. Renz, S. Valencia, Sn-zeolite beta as a heterogeneous chemoselective catalyst for Baeyer-Villiger oxidations, Nature 412 (2001) 423-425. DOI:10.1038/35086546.

[9] U. R. Pillai, E. Sahle-Demessie, Sn-exchanged hydrotalcites as catalysts for clean and selective Baeyer–Villiger oxidation of ketones using hydrogen peroxide, J. Mol. Catal. A 191 (2003) 93-100. DOI:10.1016/S1381-1169(02)00347-3.

[10] C. Jimenaz-Sanchidrian, J. M. Hidalgo, J. R. Ruiz, Baeyer–Villiger oxidation of cyclohexanone with hydrogen peroxide/benzonitrile over hydrotalcites as catalysts, Appl. Catal. A 312 (2006) 86-94. DOI:10.1016/j.apcata.2006.06.031.

[11] T. Yamada, K. Takahashi, K. Kato, T. Takai, S. Inoki, T. Mukaiyama, The Baeyer-Villiger Oxidation of Ketones Catalyzed by Nickel(II) Complexes with Combined Use of Molecular-Oxygen and Aldehyde, Chem. Lett. 20 (1991) 641-644. DOI:10.1246/cl.1991.641.

[12] J. M. Thomas, Design and Application of Single-Site Heterogeneous Catalysts, Imperial College Press, London, 2012, pp. 141–145.

[13] K. Pamin, J. Połtowicz, M. Prończuk, J. Kryściak-Czerwenka, R. Karcz, E. M. Serwicka, Keggin-Type Heteropoly Salts as Bifunctional Catalysts in Aerobic Baeyer-Villiger Oxidation, Materials 11 (2018) 1208-1218. DOI:10. 3390/ma11071208.

[14] D. Lakk-Bogath, G. Speier, J. Kaizer, Oxoiron(IV)-mediated Baeyer-Villiger oxidation of cyclohexanones generated by dioxygen with co-oxidation of aldehydes, New J. Chem. 39 (2015) 8245–8248. DOI:10.1039/C5NJ02093J.

[15] Y. Ma, Z. Liang, S. Feng, Y. Zhang, Baeyer–Villiger oxidation of cyclohexanone by molecular oxygen with Fe–Sn–O mixed oxides as catalysts, Appl. Organometal. Chem. 29 (2015) 450-455. https://doi.org/10.1002/aoc.3314. DOI:10.1007/s10562-016-1823-5.

[16] W. Zhou, Y. Chen, J. Qian, F. Sun, M. He, Copper Tetrasulfophthalocyanine Intercalated Hydrotalcite as an Efficient Bifunctional Catalyst for the Baeyer–Villiger Oxidation, Catal. Lett. 146 (2016) 2157-2164. DOI:10.1007/s10562-016-1823-5.

[17] W. Zhou, P. Tian, F. Sun, M. He, Z. Chen, Efficient Catalysis of the Aerobic.Baeyer–Villiger Oxidation over a Bifunctional Catalyst Based on Cobalt Tetraphenylporphyrin Intercalated into Zn2Al Hydrotalcite, Asian J. Org. Chem. 4 (2015) 33-37.

DOI:10.1002/ajoc.201402224.

[18] T. Kawabata, N. Fujisaki, T. Shishido, K. Nomura, T. Sano, K. Takehira, Improved Fe/Mg-Al hydrotalcite catalyst for Baeyer–Villiger oxidation of ketones with molecular oxygen and benzaldehyde, J. Mol. Catal. A 253 (2006) 279–289. DOI:10.1016/j.molcata. 2006.03.077.

[19] H. Subramanian, E. G. Nettleton, S. Bughi, R. T. Koodali, Baeyer–Villiger oxidation of cyclic ketones using Fe containing MCM-48 cubic mesoporous materials, J. Mol. Catal. A 330 (2010) 66-72. DOI:10.1016/j.molcata.2010.07.003.

[20] T. Kawabata, Y. Ohishi , S. Itsuki, N. Fujisaki, T. Shishido, K. Takaki, Q. Zhang, Y. Wang, K. Takehira, Iron-containing MCM-41 catalysts for Baeyer–Villiger oxidation of ketones using molecular oxygen and benzaldehyde, J. Mol. Catal. A 236 (2005) 99–106. DOI:10.1016/j.molcata.2005.03.027.

[21] A. Thangaraj, S. Sivasanker, P. Ratnasamy, Catalytic properties of crystalline titanium silicalites III. Ammoximation of cyclohexanone, J. Catal. 131 (1991) 394-400. DOI:10.1016/0021-9517(91)90274-8.

[22] B. Kraushaar, J.H.C. van Hooff, A new method for the preparation of titanium-silicalite (TS-1), Catal. Lett. 1 (1988) 81-84. DOI:10.1007/BF00772769.

[23] S. Dzwigaj, M. J. Peltre, P. Massiani, A. Davidson, M. Che, T. Sen, S. Sivasanker, Incorporation of vanadium species in a dealuminated β zeolite, Chem. Commun. 1 (1998) 87-88. DOI:10.1039/A704556E.

[24] S. Dzwigaj, M. Matsuoka, R. Franck, M. Anpo, M. Che, Synthesis and Structural Characterization of MWW Type Zeolite ITQ-1, the Pure Silica Analog of MCM-22 and SSZ-25, J. Phys. Chem. B 102 (1998) 6309-6312. DOI:10.1021/jp972319k.

[25] S. Dzwigaj, M. Che, Incorporation of Co(II) in Dealuminated BEA Zeolite at Lattice Tetrahedral Sites Evidenced by XRD, FTIR, Diffuse Reflectance UV−Vis, EPR, and TPR, J. Phys. Chem. B 110 (2006) 12490-12493. DOI:10.1021/jp0623387.

[26] J. Janas, T. Machej, J. Gurgul, R.P. Socha, M. Che, S. Dzwigaj, Effect of Co content on the catalytic activity of CoSiBEA zeolite in the selective catalytic reduction of NO with ethanol:Nature of the cobalt species, Appl. Catal. B 75 (2007) 239-248. DOI:10.1016/j.apcatb.2007.07.029.

[27] S. Dzwigaj, J. Janas, T. Machej, M. Che, Selective catalytic reduction of NO by alcohols on Co- and Fe-Siβ catalysts, Catal. Today 119 (2007) 133-136. DOI:10.1016/j.cattod.2006.08.055.

[28] S. Dzwigaj, J. Janas, J. Mizera, J. Gurgul, R.P. Socha, M. Che, Incorporation of Copper in SiBEA Zeolite as Isolated Lattice Mononuclear Cu(II) Species and its Role in Selective Catalytic Reduction of NO by Ethanol, Catal. Lett. 126 (2008) 36-42. DOI:10.1007/s10562-008-9675-2.

[29] J. P. Nogier, Y. Millot, P. P. Man, T. Shishido, M. Che, S. Dzwigaj, Probing the Incorporation of Ti(IV) into the BEA Zeolite Framework by XRD, FTIR, NMR, and DR UV−jp810722bis, J. Phys. Chem. C 113 (2009) 4885-4889. DOI:10.1021/jp8099829.

[30] J. P. Nogier, Y. Millot, P.P. Man, C. Methivier, M. Che, S. Dzwigaj, Nature, Environment and Quantification of Titanium Species in TiSiBEA Zeolites Investigated by XRD, NMR, DR UV−Vis and XPS, Catal. Lett. 130 (2009) 588-592. DOI:10.1007/s10562-009-9960-8.

[31] R. Baran, T. Onfroy, S. Casale, S. Dzwigaj, Introduction of Co into the Vacant T-Atom Sites of SiBEA Zeolite as Isolated Mononuclear Co Species, J. Phys. Chem. C 118 (2014) 20445-20451. DOI:10.1021/jp506375v.

[32] R. Baran, J.-M. Krafft, T. Onfroy, T. Grzybek, S. Dzwigaj, Influence of the nature and environment of cobalt on the catalytic activity of Co-BEA zeolites in selective catalytic

reduction of NO with ammonia, Micropor. Mesopor. Mater. 225 (2016) 515-523. DOI:10.1016/j.micromeso.2015.12.061.

[33] E. Bourgeat Lami, F. Fajula, D. Anglerat, T. des Courières, Single step dealumination of zeolite beta precursors for the preparation of hydrophobic adsorbents, Micropor. Mater. 1 (1993) 237-245. DOI:10.1016/0927-6513(93)80067-5.

[34] A. Janin, M. Maache, J.C. Lavalley, J.F. Joly, F. Raatz, N. Szydlowski, FT i.r. study of the silanol groups in dealuminated HY zeolites: Nature of the extraframework debris, Zeolites 11 (1991) 391-396. DOI:10.1016/0144-2449(91)80308-M.

[35] S. Dzwigaj, P. Masiani, A. Davidson, M. Che, Role of silanol groups in the incorporation of V in β zeolite, J. Mol. Catal. A 155 (2000) 169-182. DOI:10.1016/S1381-1169(99)00332-5.

[36]. Z.Yu, A. Zheng, Q. Wang, Lei Chen, J. Xu, J.-P. Amoureux, F. Deng, Insights into the Dealumination of Zeolite HY Revealed by Sensitivity-Enhanced 27Al DQ-MAS NMR Spectroscopy at High Field, Angew. Chem. Int. Ed. 49 (2010) 8657–8661, DOI: 10.1002/anie.201004007

[37]. P. Shestakova, C. Martineau, V. Mavrodinovaa, M. Popova, Solid state NMR characterization of zeolite beta based drug formulations containing Ag and sulfadiazine, RSC Adv. 5 (2015) 81957–81964, DOI: 10.1039/c5ra15097c

[38]. F. Deng, Y. Du, C. Ye, J. Wang, T. Ding, H. Li, Acid Sites and Hydration Behavior of Dealuminated Zeolite HZSM-5: A High-Resolution Solid State NMR Study, J. Phys. Chem. 99 (1995) 15208–15214, DOI: 10.1021/j100041a041

[39]. M. Gackowski, J. Podobinski, E. Broclawik, J. Datka, IR and NMR Studies of the Status of Al and Acid Sites in Desilicated Zeolite Y, Molecules 25 (2020) 31, DOI:10.3390/molecules25010031

[40]. N. Malicki, P. Beccat, P. Bourges, C. Fernandez, A.-A. Quoineaud, L. J. Simon, F. Thibault-Starzyk, Studies in Surface Science and Catalysis 170 (2007) 762-770, DOI: 10.1016/S0167-2991(07)80918-9

[41] C. A. Fyfe, H. Strobl, G. T. Kokotailo, C. T. Pasztor, G. E. Barlow, S. Bradley, Correlations between lattice structures of zeolites and their 29Si MAS n.m.r. spectra: zeolites KZ-2, ZSM-12, and Beta, Zeolites 8 (1988) 132-136. DOI:10.1016/S0144-2449(88)80079-4.

[42] C. Pazé, A. Zecchina, S. Spera, A. Cosma, E. Merlo, G. Spano, G. Girotti, Comparative IR and 1H-MAS NMR study of adsorption of CD_3CN on zeolite H-β: evidence of the presence of two families of bridged Bronsted sites, PhysChemChemPhys 1 (1999) 2627-2629. DOI:10.1039/A902621E.

[43] L.W. Beck, J.F. Haw, Multinuclear NMR Studies Reveal a Complex Acid Function for Zeolite Beta, J. Phys. Chem. 99 (1995) 1076-1079. DOI:10.1021/j100004a004.

[44] L.W. Beck, J.L. White, J.F. Haw, 1H{27Al} Double-Resonance Experiments in Solids: An Unexpected Observation in the 1H MAS Spectrum of Zeolite HZSM-5, J. Am. Chem. Soc. 116 (1994) 9657-9661. DOI:10.1021/ja00100a034.

[45] G.I. Woolery, L.B. Alemany, R.M. Dessau, A.W. Chester, Spectroscopic evidence for the presence of internal silanols in highly siliceous ZSM-5, Zeolites 6 (1986) 14-16. DOI:10.1016/0144-2449(86)90005-9.

[46] A. Zecchina, S. Bordiga, G. Spoto, L. Marchese, G. Petrini, G. Leofanti, M. Padovan, Silicalite characterization. 2. IR spectroscopy of the interaction of carbon monoxide with internal and external hydroxyl groups, J. Phys. Chem. 96 (1992) 4991-4997. DOI:10.1021/j100191a048.

[47] G.E. Maciel, P.D. Ellis, in: Bell AT, Pines A (Eds.), NMR Techniques in Catalysis, Deker, New York, 1994, p. 231.

[48] S. Klein, B.M.Weckhuysen, J.A.Martens, W.F.Maier, P.A.Jacobs, Homogeneity of Titania-Silica Mixed Oxides: On UV-DRS Studies as a Function of Titania Content, J. Catal. 163 (1996) 489-491. DOI:10.1006/jcat.1996.0350.

[49] J. Klaas, G. Schulz-Ekloff, N. I. Jaeger, UV−Visible Diffuse Reflectance Spectroscopy of Zeolite-Hosted Mononuclear Titanium Oxide Species, J. Phys. Chem. B 101 (1997) 1305-1311. DOI:10.1021/jp9627133.

[50] L. Marchese, T. Maschmeyer, E. Gianotti, S. Coluccia, J. M. Thomas, Probing the Titanium Sites in Ti−MCM41 by Diffuse Reflectance and Photoluminescence UV−Vis Spectroscopies, J. Phys. Chem. B 101 (1997) 8836-8838. DOI:10.1021/jp971963w.

[51] A. Carati, C. Flego, E. Previde Massara, R. Millini, L. Carluccio, W. O. Parker Jr., G. Bellussi, Stability of Ti in MFI and Beta structures: a comparative study, Micropor. Mesopor. Mater. 30 (1999) 137-144. DOI:10.1016/S1387-1811(99)00018-9.

[52] K. Lin, P.P. Pescarmona, H. Vandepitte, D. Liang, G.Van Tendeloo, P. A. Jacobs, Synthesis and catalytic activity of Ti-MCM-41 nanoparticles with highly active titanium sites, J. Catal. 254 (2008) 64-70. DOI:10.1016 /j.jcat.2007.11.017.

[53] P. Boroń, L. Chmielarz, J. Gurgul, K. Łątka, T. Shishido, J.-M. Krafft, S. Dzwigaj, BEA zeolite modified with iron as effective catalyst for N_2O decomposition and selective reduction of NO with ammonia, Appl. Catal. B 138–139 (2013) 434-445. DOI:10.1016/j.apcatb.2013.03.022.

[54] P. Boroń, L. Chmielarz, J. Gurgul, K. Łątka, B. Gil, J.-M. Krafft, S. Dzwigaj, The influence of the preparation procedures on the catalytic activity of Fe-BEA zeolites in SCR of NO with ammonia and N_2O decomposition, Catal. Today 235 (2014) 210–225.
DOI:10.1016/j.cattod.2014.03.018.

[55] I. Kocemba, J. Rynkowski, J. Gurgul, R. P. Socha, K. Łątka, J.-M. Krafft, S. Dzwigaj, Nature of the active sites in CO oxidation on FeSiBEA zeolites, Appl. Catal. A 519 (2016) 16–26. DOI:10.1016/j.apcata.2016. 03.025.

[56] M. S. Kumar, M. Schwidder, W. Grünert, U. Bentrup, A. Brückner, Selective reduction of NO with Fe-ZSM-5 catalysts of low Fe content: Part II. Assessing the function of different Fe sites by spectroscopic in situ studies, J. Catal. 239 (2006) 173-186. DOI:10.1016/j.jcat.2006.01.024.

[57] K. Arishtirova, P. Kovacheva, A. Predoeva, Activity and basicity of BaO modified zeolite and zeolite-type catalysts, Appl. Catal. A 243 (2003) 191-196. DOI: 10.1016/S0926-860X(02)00544-6

[58] P. Kovacheva, K. Arishtirova, A. Predoeva, Basic zeolite and zeolite-type catalysts for the oxidative methylation of toluene with methane, React. Kin. Catal. Lett. 79 (2003) 149-155. DOI: 10.1016/S0926-860X(02)00544-6.

[59] L. P. Oleksenko, Characteristics of Active Site Formation in Co-Containing Catalysts for CO Oxidation on Chemically Different Supports, Theoretical and Experimental Chemistry 40 (2004) 331-336. DOI: 10.1023/B:THEC. 0000049081.04366.a7.

[60] W. Grünert, R. Schlögl, Photoelectron Spectroscopy of Zeolites, Molecular Sieves 4 (2004) 467-515. DOI: 10.1007/b94241.

[dataset] [61] A. V. Naumkin, A. Kraut-Vass, S. W. Gaarenstroom, and C. J. Powell, NIST X-ray Photoelectron Spectroscopy Database. http://srdata.nist. gov/xps/. DOI: 10.18434/T4T88K.

[62] J. Janas, J. Gurgul, R. P. Socha, S. Dzwigaj, Effect of Cu content on the catalytic activity of CuSiBEA zeolite in the SCR of NO by ethanol: Nature of the copper species, Appl. Catal. B 91 (2009) 217-224. DOI: 10.1016/j.apcatb.2009.05.028.

[63] J. Gurgul, K. Łątka, I. Hnat, J. Rynkowski, S. Dzwigaj, Identification of iron species in FeSiBEA by DR UV–vis, XPS and Mössbauer spectroscopy: Influence of Fe content, Micropor. Mesopor. Mater. 168 (2013) 1–6. DOI: 10.10 16 /j.micromeso.2012.09.015.

[64] P. Boroń, L. Chmielarz, J. Gurgul, K. Łątka, B. Gil, B. Marszałek, S. Dzwigaj, Influence of iron state and acidity of zeolites on the catalytic activity of FeHBEA, FeHZSM-5 and FeHMOR in SCR of NO with NH_3 and N_2O decomposition, Micropor. Mesopor. Mater. 203 (2015) 73–85. DOI: 10.1016/j.micromeso.2014.10.023.

[65] D. Sun, Y. Huang, B. Han, G. Yang, Ti−Si Mixed Oxides Prepared by Polymer in Situ Sol−Gel Chemistry with the Aid of CO_2, Langmuir 22 (2006) 4793-4798. DOI: 10.1021/la053172o.

[66] A. Y. Stakheev, E. S. Shpiro, J. Apijok, XPS and XAES study of titania-silica mixed oxide system, J. Phys. Chem. 97 (1993) 5668-5672. DOI: 10.1021/j100123a034.

[67] G. M. Ingo, S. Dirè, F. Babonneau, XPS studies of SiO_2-TiO_2 powders prepared by sol-gel process, Appl. Surf. Sci. 70-71 (1993) 230-234. DOI: 10.1016/0169-4332(93)90433-C.

[68] G. Lassaletta, A. Fernandez, J. P. Espinos, A. R. Gonzalez-Elipe, Spectroscopic characterization of quantum-sized TiO_2 supported on silica: influence of size and TiO_2-SiO_2 interface composition, J. Phys. Chem. 99 (1995) 1484–1490. DOI: 10.1021/j100005a019.

[69] J. Mayer, E. Garfunkel. T. E. Madey, U. Diebold, Titanium and reduced titania overlayers on titanium dioxide(110), J. Electron Spectrosc. Relat. Phenom. 73 (1995) 1-11. DOI: 10.1016/0368-2048(94)02258-5.

[70] M. Biesinger, L. Lau, A. Gerson, R. Smart, Resolving surface chemical states in XPS analysis of first row transition metals, oxides and hydroxides: Sc, Ti, V, Cu and Zn, Appl. Surf. Sci. 257 (2010) 887-898. DOI: 10.1016/j.apsusc.2010.07.086.

[71] J. Janas, J. Gurgul, R.P. Socha, J. Kowalska, K. Nowińska, T. Shishido, M. Che, S. Dzwigaj, Influence of the Content and Environment of Chromium in CrSiBEA Zeolites on the

Oxidative Dehydrogenation of Propane, J. Phys. Chem. C 113 (2009) 13273-13281. DOI: 10.1021/jp809733s.

[72] M. F. Brest, R. A. Condrate, A raman study of TiO_2-SiO_2 glasses prepared by sol-gel processes, J. Mater. Sci. Lett. 4 (1985) 994-998. DOI: 10.1007/BF00721102.

[73] V. Smeets, C. Boissiere, C. Sanchez, E. M. Gaigneaux, E. Peeters, B. F. Sels, M. Dusselier, D. P. Debecker, Chem. Mater. 2019, 31, 1610−1619. DOI: 10.1021/acs.chemmater.8b04843

[74] M. R. Boccuti, K. M. Rao, A. Zecchina, G. Leofanti, G. Petrini, Spectroscopic Characterization of Silicalite and Titanium-Silicalite, Stud. Surf. Sci. Catal. 48 (1989) 133-144. DOI: 10.1016/S0167-2991(08)60677-1.

[75] K. Kosuge, P. S. Singh, Titanium-Containing Porous Silica Prepared by a Modified Sol−Gel Method, J. Phys. Chem. B 103 (1999) 3563-3569. DOI: 10.1021/jp9847843.

[76] J. Chastain, R. C. King, Handbook of X-ray Photoelectron Spectroscopy, Physical Electronics, Inc., Minneapolis, 1995.

[77] M. Trejda, M. Ziolek, Y. Millot, K. Chalupka, M. Che, S. Dzwigaj, Methanol oxidation on VSiBEA zeolites: Influence of V content on the catalytic properties, J. Catal. 281 (2011) 169-176. DOI: 10.1016/j.jcat.2011.04.013.

[78] J. Janas, J. Gurgul, R.P. Socha, T. Shishido, M. Che, S. Dzwigaj, Selective catalytic reduction of NO by ethanol: Speciation of iron and “structure–properties” relationship in FeSiBEA zeolite, Appl. Catal. B 91 (2009) 113-122. DOI: 10.1016/j.apcatb.2009.05.013.

[79] S. Dzwigaj, T. Shishido, State of Chromium in CrSiBEA Zeolite Prepared by the Two-Step Post-synthesis Method: XRD, FTIR, UV−Vi□, EPR, TPR, □□d XAS Studie□, J. Phy□ Chem. C 112 (2008) 5803-5809. DOI: 10.1021/jp711086m.

[80] S. Dzwigaj, J.-P. Nogier, M. Che, M. Saito, T. Hosokawa, E. Thouverez, M. Matsuoka, M. Anpo, Influence of the Ti content on the photocatalytic oxidation of 2-propanol and CO on TiSiBEA zeolites, Catal. Commun. 19 (2012) 17–20. DOI: 10.1016/j.catcom.2011.12.010.

[81] C. A. Emeis, Determination of Integrated Molar Extinction Coefficients for Infrared Absorption Bands of Pyridine Adsorbed on Solid Acid Catalysts, J. Catal. 141 (1993) 347-354. DOI: 10.1006/jcat.1993.1145

[82] M. Boronat, P. Concepción, A. Corma, M. Renz, Peculiarities of Sn-Beta and potential industrial applications, Catal. Today 121 (2007) 39–44. DOI: 10.1016/j.cattod.2006.11.010.

[83] S. Dzwigaj, J. Janas, W. Rojek, L. Stievano, F.E. Wagner, F. Averseng, M. Che, Effect of iron impurities on the catalytic activity of BEA, MOR and MFI zeolites in the SCR of NO by ethanol, Appl. Catal. B 86 (2009) 45-52. DOI: 10.1016/j.apcatb.2008.07.017.

[84] A. Corma, Attempts to Fill the Gap Between Enzymatic, Homogeneous, and Heterogeneous Catalysis, Catal. Rev. 46 (2004) 369–417. DOI: 10.1081/CR-200036732.

[85] W.V. Doering, E. Dorfman, Mechanism of the Peracid-Ketone Ester Conversion. Analysis of Organic Compounds for Oxygen-18[1], J. Am. Chem. Soc., 75 (1953) 5595–5598. DOI: 10.1021/ja01118a035.

[86] R.A. Sheldon, J.K. Kochi, in R.A. Sheldon, Metal-Catalyzed Oxidations of Organic Compounds, Academic Press, New York 1981, p. 78.

[87] I.W.C.E. Arends, R.A. Sheldon, Activities and stabilities of heterogeneous catalysts in selective liquid phase oxidations: recent developments, Applied Catalysis A: General 212 (2001) 175–187. DOI: 10.1016/S0926-860X(00)00855-3.

Table 1. The BE values (eV) and relative areas of components (%) of Ti $2p_{3/2}$ core excitations obtained for Ti_xSiBEA samples. The spin-orbit splitting Δ (eV) of each doublet is also listed.

Sample	Ti-O-Ti	Ti-O-Si	Δ_A	Δ_B
$Ti_{4.3}SiBEA$	459.9 (49.1)	460.4 (50.9)	5.0	5.9
$Ti_{2.6}SiBEA$	459.7 (38.5)	460.6 (61.5)	5.0	5.8
$Ti_{2.0}SiBEA$	459.1 (13.0)	460.3 (87.0)	4.7	5.4
$Ti_{1.1}SiBEA$	458.8 (10.6)	460.1 (89.4)	4.8	5.4
$Ti_{0.8}SiBEA$	458.2 (8.8)	460.4 (91.2)	4.8	5.0

Table 2. The number of Brønsted and Lewis acid sites in HAlBEA, SiBEA and Ti_xSiBEA zeolites.

Samples	Brønsted acid sites[a] [µmol g^{-1}]	Lewis acid sites [µmol g^{-1}]
HAlBEA	235	117
SiBEA	3	1
$Ti_{0.8}$SiBEA	4	2
$Ti_{1.1}$SiBEA	8	5
$Ti_{2.0}$SiBEA	10	5
$Ti_{2.6}$SiBEA	17	19
$Ti_{4.3}$SiBEA	5	15

[a] Quantification of number of acidic sites in zeolite was done as reported earlier by Emeis [80].

Table 3. Liquid-phase Baeyer–Villiger oxidation of cyclohexanone to ε-caprolactone in the oxygen-aldehyde system on SiBEA and Ti_xSiBEA zeolites at 313 K for 5 h at atmospheric pressure.

Catalyst	Conversion [%]	ε-caprolactone selectivity [%]	TON[a]
SiBEA	18.4	53.3	-
$Ti_{0.8}$SiBEA	38.3	74.5	78
$Ti_{1.1}$SiBEA	64.3	65.2	130
$Ti_{2.0}$SiBEA	77.4	98.6	157
$Ti_{2.0}$SiBEA[b]	77.6	98.5	157
$Ti_{2.6}$SiBEA	71.8	63.6	148
$Ti_{2.6}$SiBEA[b]	71.3	63.1	145
$Ti_{4.3}$SiBEA	37.3	83.4	76

[a] moles of reactant converted per mole of titanium

[b] second run

Figure captions

Figure 1. Oxidation of cyclohexanone to ε-caprolactone at 313 K for 5 h at atmospheric pressure.

Figure 2. X-ray diffractograms of HAlBEA, SiBEA and Ti_xSiBEA zeolite samples as prepared, recorded at room temperature and in ambient atmosphere.

Figure 3. FT-IR spectra of HAlBEA, SiBEA and Ti_xSiBEA zeolites calcined at 773 K for 3 h in flowing air followed by outgassing at 573 K (10^{-3} Pa) for 2 h, recorded at room temperature.

Figure 4. ^{27}Al MAS NMR spectra of HAlBEA, SiBEA and Ti_xSiBEA zeolites as prepared, recorded at room temperature in 4 mm (external diameter) zirconia rotor.

Figure 5. ^{29}Si MAS NMR spectra of HAlBEA, SiBEA and Ti_xSiBEA zeolites as prepared, recorded at room temperature in 7 mm (external diameter) zirconia rotor.

Figure 6. ^{1}H - ^{29}Si CP MAS NMR spectra of HAlBEA, SiBEA and TiSiBEA zeolites as prepared, recorded at room temperature in 7 mm (external diameter) zirconia rotor.

Figure 7. ^{1}H MAS NMR spectra of AlBEA, SiBEA and Ti_xSiBEA zeolites as prepared, recorded at room temperature in 4 mm (external diameter) zirconia rotor.

Figure 8. DR UV-vis spectra of Ti_xSiBEA zeolites as prepared, recorded at room temperature and in ambient atmosphere.

Figure 9. XPS of Ti_xSiBEA zeolites as prepared, recorded at room temperature.

Figure 10. FTIR spectra of HAlBEA, SiBEA, $Ti_{0.8}SiBEA$, $Ti_{1.1}SiBEA$, $Ti_{2.0}SiBEA$, $Ti_{2.6}SiBEA$ and $Ti_{4.3}SiBEA$ zeolites after calcination at 773 K for 3 h in flowing air followed by outgassing at 573 K (10^{-3} Pa) for 2 h, adsorption of pyridine at room temperature, its desorption for 2 h at 423 K and spectra recording at room temperature.

Figure 11. Variation of the perbenzoic acid concentration as a function of reaction time.

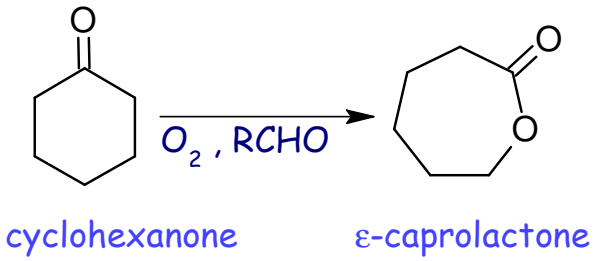
O
O
O
O2 , RCHO
cyclohexanone
ε-caprolactone

Fig. 1

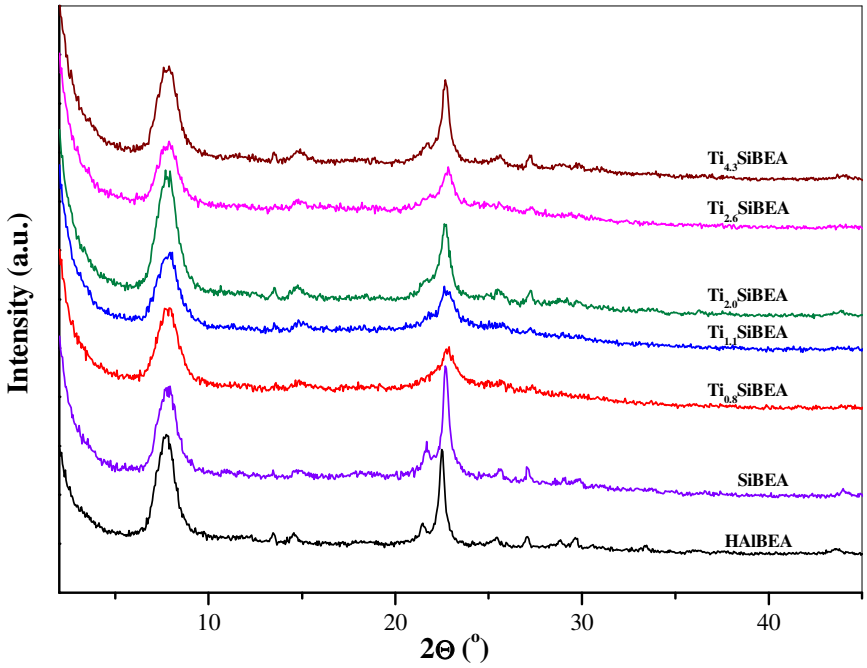
Intensity (a.u.)
Ti4.3SiBEA
Ti2.6SiBEA
Ti2.0SiBEA
Ti1.1SiBEA
Ti0.8SiBEA
SiBEA
HAlBEA
10
20
30
40
2Θ (°)

Fig. 2

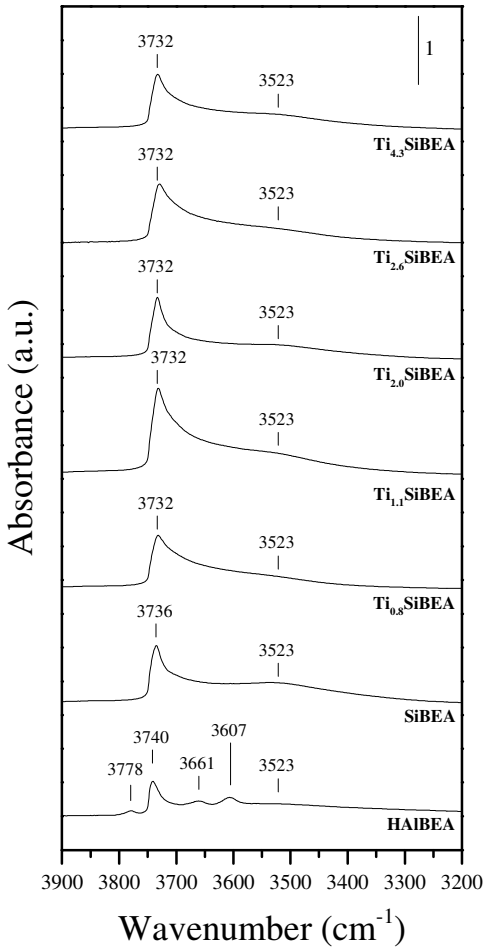
3732
1
3523
Ti4.3SiBEA
3732
3523
Ti2.6SiBEA
3732
3523
Ti2.0SiBEA
3732
3523
Ti1.1SiBEA
3732
3523
Ti0.8SiBEA
3736
3523
SiBEA
3740
3607
3778
3661
3523
HAlBEA
Absorbance (a.u.)
3900 3800 3700 3600 3500 3400 3300 3200
Wavenumber (cm-1)

Fig. 3

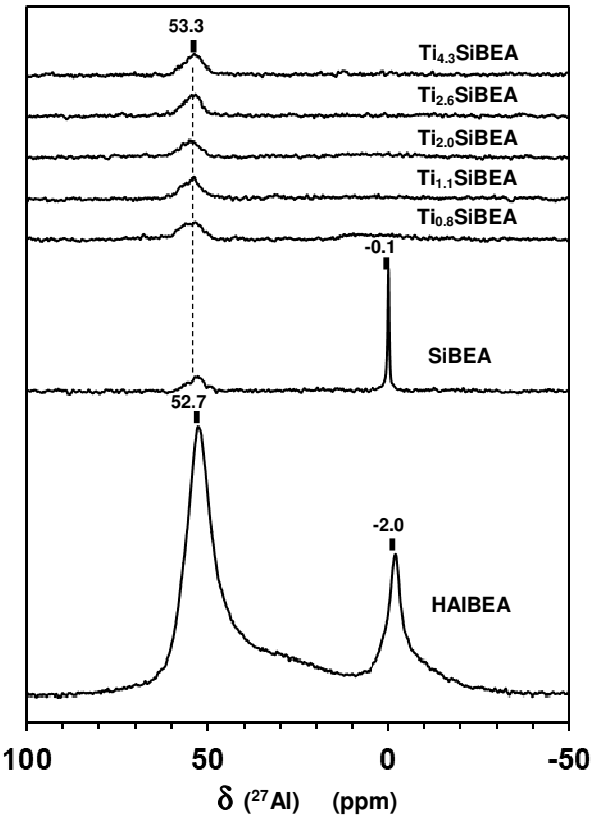
53.3
Ti4.3SiBEA
Ti2.6SiBEA
Ti2.0SiBEA
Ti1.1SiBEA
Ti0.8SiBEA
-0.1
SiBEA
52.7
-2.0
HAlBEA
100
50
0
-50
δ (27Al) (ppm)

Fig. 4

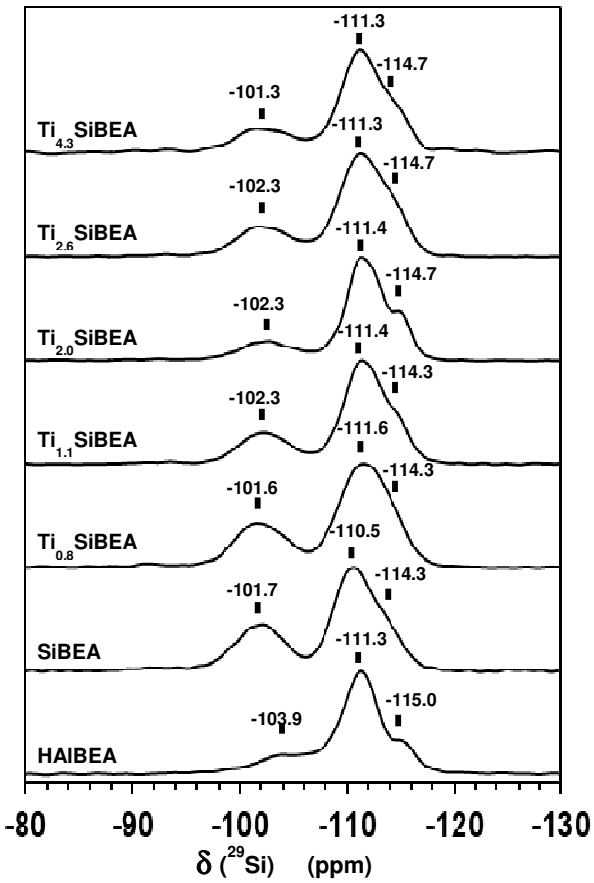
-111.3
-114.7
-101.3
Ti4.3SiBEA
-111.3
-114.7
-102.3
Ti2.6SiBEA
-111.4
-114.7
-102.3
Ti2.0SiBEA
-111.4
-114.3
-102.3
Ti1.1SiBEA
-111.6
-114.3
-101.6
Ti0.8SiBEA
-110.5
-114.3
-101.7
SiBEA
-111.3
-115.0
-103.9
HAlBEA
-80
-90
-100
-110
-120
-130
δ (29Si) (ppm)

Fig. 5

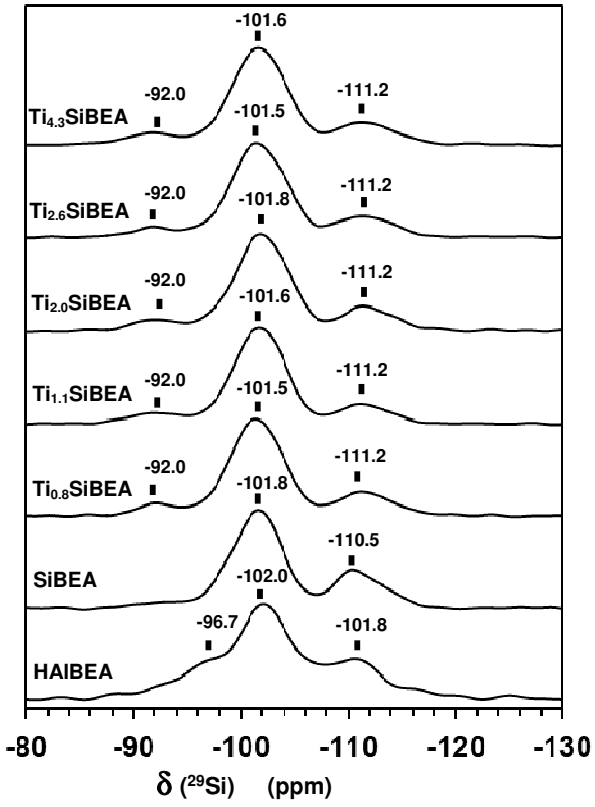
-101.6
-92.0
-111.2
Ti4.3SiBEA
-101.5
-92.0
-111.2
Ti2.6SiBEA
-101.8
-92.0
-111.2
Ti2.0SiBEA
-101.6
-92.0
-111.2
Ti1.1SiBEA
-101.5
-92.0
-111.2
Ti0.8SiBEA
-101.8
-110.5
SiBEA
-102.0
-96.7
-101.8
HAlBEA
-80
-90
-100
-110
-120
-130
δ (29Si) (ppm)

Fig. 6

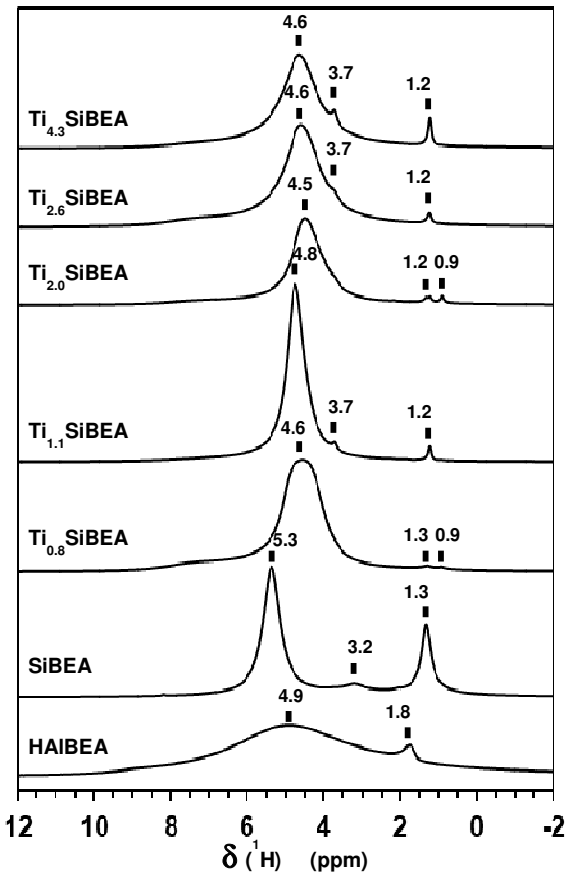
4.6
3.7
1.2
Ti4.3SiBEA
4.6
3.7
1.2
Ti2.6SiBEA
4.5
4.8
1.2 0.9
Ti2.0SiBEA
3.7
1.2
Ti1.1SiBEA
4.6
1.3 0.9
Ti0.8SiBEA
5.3
1.3
3.2
SiBEA
4.9
1.8
HAlBEA
12 10 8 6 4 2 0 -2
δ (1H) (ppm)

Fig. 7

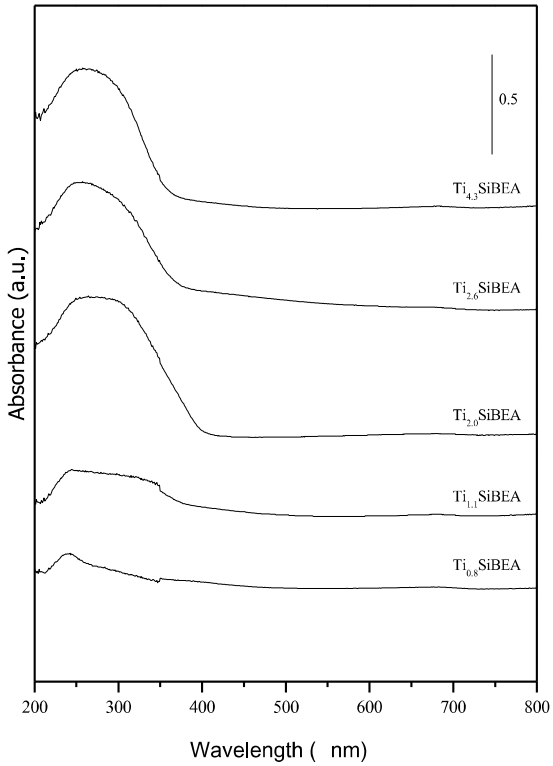
0.5
Ti4.3SiBEA
Ti2.6SiBEA
Ti2.0SiBEA
Ti1.1SiBEA
Ti0.8SiBEA
Absorbance (a.u.)
200
300
400
500
600
700
800
Wavelength (nm)

Fig. 8

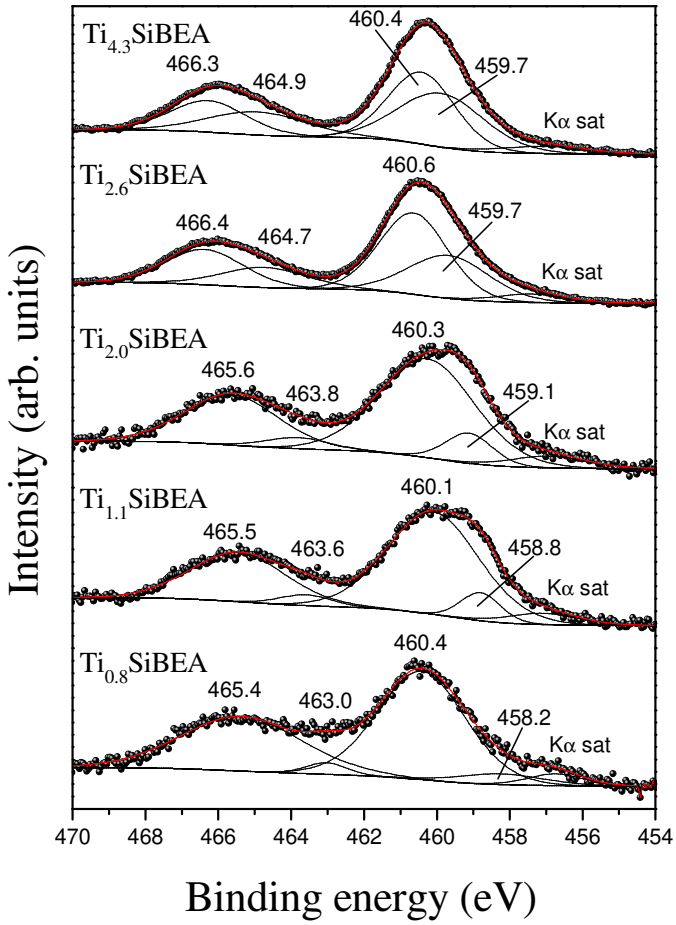
Ti4.3SiBEA
460.4
466.3
464.9
459.7
Kα sat
Ti2.6SiBEA
460.6
466.4
464.7
459.7
Kα sat
Ti2.0SiBEA
460.3
465.6
463.8
459.1
Kα sat
Ti1.1SiBEA
460.1
465.5
463.6
458.8
Kα sat
Ti0.8SiBEA
460.4
465.4
463.0
458.2
Kα sat
Intensity (arb. units)
470
468
466
464
462
460
458
456
454
Binding energy (eV)

Fig. 9

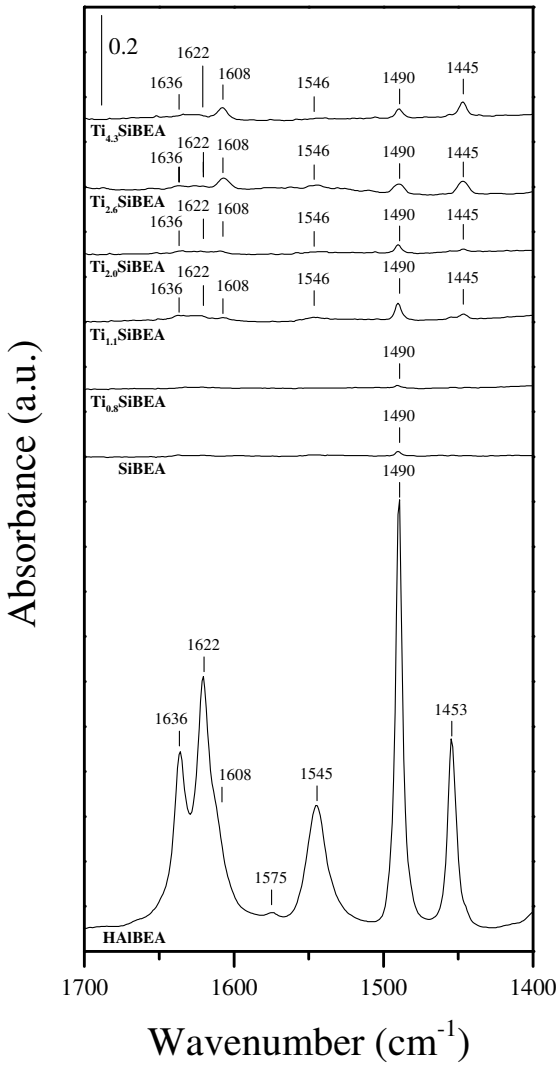
0.2
1622
1636
1608
1546
1490
1445
Ti4.3SiBEA
Ti2.6SiBEA
Ti2.0SiBEA
Ti1.1SiBEA
Ti0.8SiBEA
SiBEA
HAlBEA
1453
1545
1575
Absorbance (a.u.)
1700
1600
1500
1400
Wavenumber (cm-1)

Fig. 10

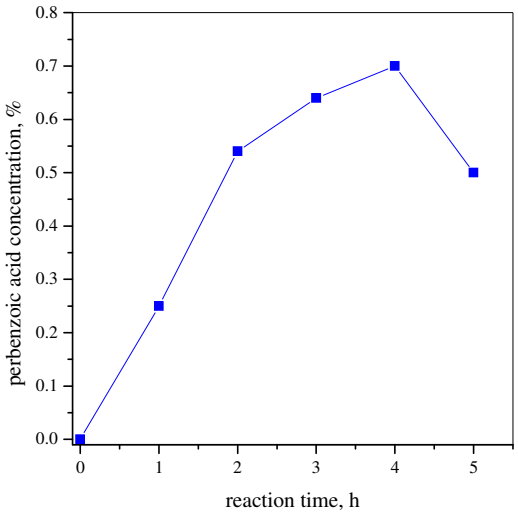
perbenzoic acid concentration, %
reaction time, h
0.0
0.1
0.2
0.3
0.4
0.5
0.6
0.7
0.8
0
1
2
3
4
5

Fig. 11

Graphical Abstract :